

The charge order transition and elastic/anelastic properties of LiMn_2O_4

This article has been downloaded from IOPscience. Please scroll down to see the full text article.

2003 J. Phys.: Condens. Matter 15 457

(<http://iopscience.iop.org/0953-8984/15/3/310>)

View [the table of contents for this issue](#), or go to the [journal homepage](#) for more

Download details:

IP Address: 171.66.16.119

The article was downloaded on 19/05/2010 at 06:29

Please note that [terms and conditions apply](#).

The charge order transition and elastic/anelastic properties of LiMn_2O_4

A Paolone^{1,4}, R Cantelli¹, G Rousse² and C Masquelier³

¹ INFN—Università di Roma ‘La Sapienza’, Dipartimento di Fisica, Piazzale Aldo Moro 2, I-00185 Roma, Italy

² Institut Laue-Langevin, BP 156, F-38042 Grenoble Cedex 9, France

³ Université de Picardie ‘Jules Verne’, Laboratoire de Réactivité et de Chimie des Solides, F-80039 Amiens Cedex, France

E-mail: Annalisa.Paolone@roma1.infn.it

Received 16 July 2002, in final form 18 November 2002

Published 13 January 2003

Online at stacks.iop.org/JPhysCM/15/457

Abstract

We studied the charge ordering transition of LiMn_2O_4 by means of anelastic spectroscopy, measuring the Young's modulus, E' , and the elastic energy loss function, Q^{-1} . Our measurements confirm the occurrence of a phase transition at 296 K on cooling, showing a large hysteresis on heating. The anelastic spectroscopy results also indicate that the transformation is characterized by the coexistence of two phases. The shape of the real part of the Young's modulus seems to indicate that the elastic constant which is more strongly affected by the transition is c_{44} , like in the case of Fe_3O_4 . The time evolution of E' in the coexistence region was measured. The characteristic time, τ , of this evolution rapidly decreases from 296 to 290 K and then increases on further cooling. This behaviour of τ can possibly be related to the temperature dependence of E' . The absolute value of the Young's modulus of LiMn_2O_4 obtained considering the effect of the porosity of the sample was estimated to be of the order of 10 GPa. Finally a new thermally activated peak, centred around 100 K at a measurement frequency of ~ 1 kHz, has been observed, which cannot be described by the Debye or Fuoss–Kirkwood model. This relaxation may be ascribed to the stress-induced jumps of charges from Mn^{3+} to Mn^{4+} sites, similarly to an analogous process found in Fe_3O_4 , or to possible small movements of the octahedra and tetrahedra composing the crystal structure.

1. Introduction

Lithium manganospinel has attracted much interest in the last few years due to their potential use as cathodes in rechargeable lithium-ion batteries and due to the occurrence of a phase

⁴ Author to whom any correspondence should be addressed.

transition around room temperature corresponding to a partial charge ordering on the Mn site, as revealed by neutron scattering measurements [1]. In the ordered phase there is an alternation of Mn^{3+} and Mn^{4+} ions, similarly to the case of magnetite, Fe_3O_4 , in which the ordering of Fe^{2+} and Fe^{3+} ions was first invoked by Verwey in 1939 [2] to explain a phase transition taking place around $T_V = 120$ K. Charge ordering phenomena have been reported both in high-temperature superconductors (HTSCs) and in colossal-magnetoresistance manganites and have been related to the peculiar physical properties of these materials. However, both in HTSCs and in manganites, many details of the charge ordered state still need to be elucidated. As regards Fe_3O_4 , only recently has its low-temperature unit cell finally been reported [3]. LiMn_2O_4 can be thought of as a prototype where diffraction spectra have elucidated many details of the charge ordered phase.

LiMn_2O_4 has the spinel crystal structure with cubic symmetry above room temperature [1]. A schematic representation of the unit cell in the cubic phase is reported in figure 1. The cubic crystal structure is the same as that of Fe_3O_4 . Differential scanning calorimetry [4], electric resistivity [4], infrared spectroscopy [5] and x-ray diffraction [6] measurements demonstrated that in LiMn_2O_4 there is a phase transition taking place at ~ 295 K on cooling with a hysteresis of about 15 K on heating. The coexistence of two phases during the transformation was first evidenced by means of x-ray diffraction measurements [6]. Below room temperature the crystal structure becomes orthorhombic; the lattice cell is a $3a \times 3a \times a$ superstructure of the cubic cell (lattice parameter $a = 8.2495$ Å) [1, 4]. In the orthorhombic phase two of the five Mn sites correspond to well defined Mn^{4+} ions and the other three sites are close to Mn^{3+} ions. The low-valence manganese ions are distributed along two types of column running parallel to [001] and surrounded by Mn^{4+} ions [1].

In the following we will report the study of elastic properties of LiMn_2O_4 from 1 to 400 K with particular attention paid to the behaviour of the Young's modulus around the charge order phase transition.

2. Experimental details

LiMn_2O_4 single crystals are not available due to the occurrence of decomposition of this material at a temperature lower than the melting point. LiMn_2O_4 powders were prepared by a solid-state reaction as illustrated elsewhere [4]. The powders were sintered for 50 h at 1073 K to maintain the oxygen stoichiometry and a bar, with dimensions of $0.9 \times 5.1 \times 30$ mm³, was cut and measurements made on it. The correct stoichiometry of the sample used in the present investigation was checked by means of redox titration [4].

The complex Young's modulus $E(\omega) = E' + iE''$, whose reciprocal is the elastic compliance $s = E^{-1}$, was measured as a function of temperature by electrostatically exciting the first or the fifth flexural mode and detecting the vibration amplitude by a frequency modulation technique. The vibration frequency, $\omega/2\pi$, is proportional to $\sqrt{E'}$, while the elastic energy loss coefficient (or reciprocal of the mechanical Q) is given by [7] $Q^{-1}(\omega, T) = E''/E' = s''/s'$, and was measured from the decay of the free oscillations or the width of the resonance peak. The imaginary part of the dynamic susceptibility s'' is related to the spectral density $J_\varepsilon(\omega, T) = \int dt e^{i\omega t} \langle \varepsilon(t)\varepsilon(0) \rangle$ of the macroscopic strain ε through the fluctuation-dissipation theorem, $s'' = (\omega V/2k_B T)J_\varepsilon$.

The measurements of E' are not absolute values, as we used a sintered porous polycrystal. However, the relative change of E' with temperature was directly obtained from our measurements, considering $\omega/2\pi$ to be proportional to $\sqrt{E'}$. In the following, we will also present an evaluation of the value of Young's modulus obtained from our measurements.

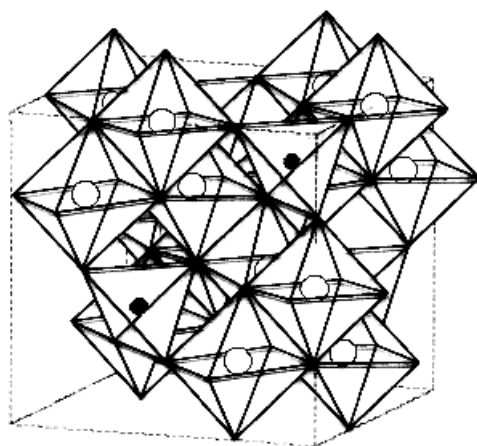


Figure 1. A schematic representation of the cubic crystal structure of LiMn_2O_4 above room temperature. Each corner of the tetrahedra and octahedra is occupied by an oxygen atom. Black and white dots represent Li and Mn ions, respectively.

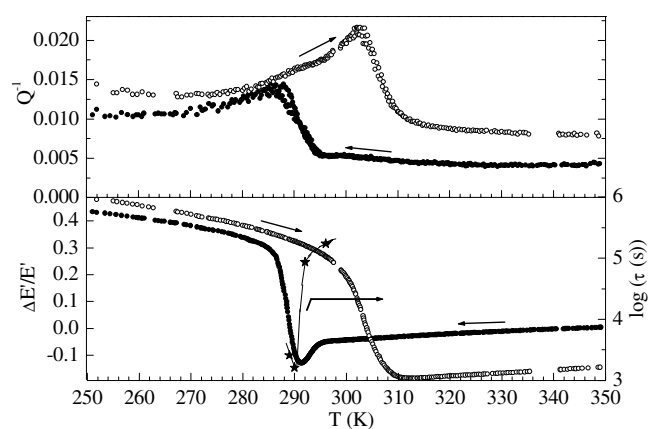


Figure 2. The elastic energy loss coefficient and the relative variation of Young's modulus of LiMn_2O_4 around the charge order transition temperature. Open and filled dots relate to measurements on heating and on cooling, respectively. Stars represent the logarithm of the time constant of the transformation. The continuous curve connecting stars is a guide for the eyes.

3. Results and discussion

3.1. The charge order transition

Anelastic spectroscopy is a powerful experimental tool for studying phase transitions involving the crystal structure, as the real part of the Young's modulus is very sensitive even to changes on a subnanometric scale in the position of atoms in the lattice. Usually, phase transitions produce intense changes of E' and peaks in E'' . These peaks are caused by the movements of the walls of the domains which are formed in the low-temperature phase. The anelastic spectra of LiMn_2O_4 on cooling and on heating at rates lower than 0.25 K min^{-1} are reported in figure 2. An abrupt change of $\Delta E'/E'$ is clearly visible on cooling, starting at 296 K; on heating, the elastic constants undergo a marked drop which starts around 300 K. At the

corresponding temperatures, the elastic energy dissipation on heating and on cooling exhibits peaks whose shift denotes a marked hysteresis. These features are ascribed to the occurrence of the phase transition. Previous anelastic measurements on LiMn_2O_4 powders [8] did not reveal any hysteresis at the transition and the anomaly of E' was detected around 230 K. This temperature is quite different from those of the present results and of the neutron scattering and resistivity study [1]. This may be due to a different stoichiometry of the sample of [8], which however the authors did not check. In fact, even small changes in Li or Mn composition strongly decrease the transition temperature and tend to suppress the hysteresis [9, 10].

In $\text{Fe}_{3-x}\text{Zn}_x\text{O}_4$ the almost vertical shape of E' for $x \sim 0$ and its progressive change to a smeared feature on heavier doping were attributed to the occurrence of a first-order transition in the undoped sample, which progressively changes to a second-order transition on doping [11]. For LiMn_2O_4 , E' undergoes an abrupt change on cooling, in agreement with a first-order transition. Also the occurrence of a hysteresis due to the phase coexistence is indicative of a first-order transition.

In the following we want to further compare the elastic properties of LiMn_2O_4 with those of Fe_3O_4 , in order to obtain information about the behaviour of the elastic properties of LiMn_2O_4 around the phase transition. In the case of Fe_3O_4 , single crystals and detailed studies on elastic constants along different crystallographic directions are available [11, 12]. The Young's modulus of Fe_3O_4 along the (111) direction and the torsion modulus along (100) present a monotonic decrease of about 10–15% with decreasing T between room temperature and 120 K, whilst both physical quantities undergo a marked increase below the transition temperature [12]. These features are closely similar to those obtained for LiMn_2O_4 on cooling in the present study. Moreover, Schwenk *et al* [11] measured the elastic constants c_{11} (the ratio between the tensile stress and the corresponding tensile strain) and c_{44} (the ratio between the shear stress and the corresponding shear strain) and the difference between c_{11} and c_{12} for a Fe_3O_4 crystal as a function of temperature. A strong softening of c_{44} from room temperature down to $T_V = 124$ K was observed, while c_{11} shows an increase of about 1% between 300 K and T_V . All the elastic constants exhibit positive steps at T_V followed by further increases with decreasing temperature. The softening of c_{44} was explained by Schwenk *et al* [11] considering a bilinear coupling of the elastic strain to an order parameter linked to the charge ordering process.

In the present study we measured the Young's modulus of a sintered polycrystal and we could not directly obtain the elastic constants along different crystallographic axes; nevertheless, some information about the behaviour of the c_{ij} s of LiMn_2O_4 around the phase transition can be obtained from the comparison with Fe_3O_4 , considering E to be linked to all c_{ij} s by a rational relationship [13]. Usually the c_{ij} s are smooth functions of temperature; however, when a phase transition occurs, all the elastic constants show a clear step, as in the case of the Fe_3O_4 crystal [11]. Correspondingly, the shape of E changes, resembling the shape of the c_{ij} s which is more strongly affected by the transformation. From the present measurements on LiMn_2O_4 and the comparison with the c_{ij} s of Fe_3O_4 , it is possible to see that on cooling the observed shape of E correspond to the change of c_{44} , whilst on heating the shape is very different, resembling that of c_{11} for Fe_3O_4 .

The abrupt change of the slope of E around 296 K on cooling is directly linked to the occurrence of the phase transition. At this temperature, in fact, the cubic phase starts transforming into the orthorhombic phase; correspondingly the relationships linking E to the c_{ij} s of a cubic sample are not valid any longer, so the shape of E is expected to suddenly change even though the c_{ij} s do not show any abrupt change at this temperature.

The coexistence of two phases in LiMn_2O_4 around room temperature has been evidenced by x-ray scattering measurements [6]. Our anelastic spectroscopy measurements confirm this.

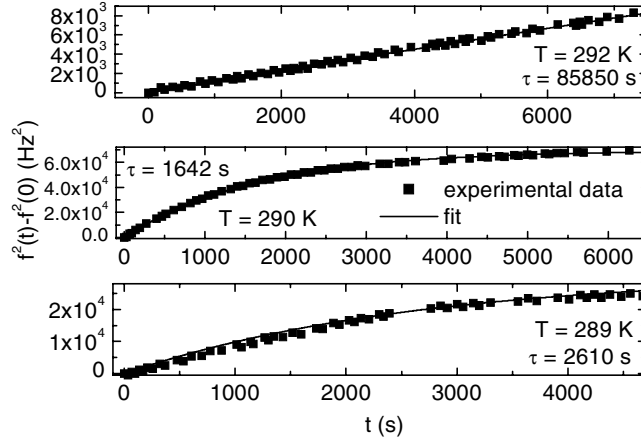


Figure 3. The time dependence of the square of the vibration frequency around the charge order transition temperature (symbols) and best-fit curves, as described in the text.

In fact, only in first-order transitions, in the coexistence region, is E expected to depend on both time, t , and temperature, T , due to the transformation of one thermodynamic phase into the other. In contrast, when a second-order transition occurs or a sample is far away from a phase transition, no dependence of E on t is expected. We could not observe any time dependence of E above 300 K, as expected, whilst we measured the time evolution of E on cooling at $T = 296, 292, 290$ and 289 K. In figure 3 the data at various temperatures are reported. The shape for the f^2 -data (which are proportional to E') could not be reproduced by a polynomial function (up to the fourth order), while it could be fitted by the following exponential law:

$$f^2(t) = f_0^2 + \Delta f^2(1 - e^{-t/\tau}).$$

In the previous formula, f_0 is the value of the vibration frequency at $t = 0$, Δf^2 is the difference between f^2 for $t \rightarrow \infty$ and $t = 0$, and τ can be thought of as a characteristic time constant of the transformation between the two phases. The use of an exponential law was motivated by a theoretical study on the kinetics of a system quenched from an initial equilibrium state with T higher than the temperature of a first-order transition, T_c , to a state with $T < T_c$ [14]. The agreement between the exponential law and the experimental data at various values of T is quite good. The change of f^2 at 296 K was very slight and very slow ($\tau > 48$ h); on lowering T , τ rapidly decreases to ~ 24 h at 292 K and to ~ 27 min at 290 K; on further cooling, τ increases to ~ 43 min at 289 K. It can be noted from figure 2 that the temperature behaviour of τ is similar to that of the Young's modulus and, implicitly, that of c_{44} . In fact E' (and c_{44}) decreases, lowering T between 296 and 292 K and increases on further cooling, even though at 290 K the E' -value is still lower than at 296 K.

Due to the resemblance of the temperature behaviours of τ and E' , it can be hypothesized that the strong decrease of the characteristic time for the transformation between the cubic and orthorhombic phases around 292 K can be attributed to the decrease of Young's modulus and, implicitly, that of c_{44} . At a microscopic level the orthorhombic phase of LiMn₂O₄ can be obtained from the cubic one by applying shear stresses to the Mn–O octahedra composing the crystal structure. A lower value of c_{44} means that a lower value of the stress is needed to change the crystal structure, so it may be thought that a shorter time is needed to transform the cubic into the orthorhombic phase in the temperature range where c_{44} is minimum.

3.2. Evaluation of the real part of the Young's modulus

In this section we present an evaluation of the absolute value of the Young's modulus of LiMn_2O_4 . As we measured a sintered polycrystal we had to consider the effect of the porosity, P , of the sample on its elastic properties. P is defined as $1 - (\rho_{exp}/\rho_{theo})$, where ρ_{exp} is the density of the measured sample and $\rho_{theo} = 4.28 \text{ g cm}^{-3}$ is the theoretical value of the density. Sugiyama *et al* [8] estimated E'_1 at 300 K from the sound velocity of a sample, with $P \sim 38\%$, assuming that the Poisson's ratio, ν , of LiMn_2O_4 had a typical value of 0.3. These authors obtained $E'_1(T = 300 \text{ K}) = 25 \text{ GPa}$ after correction for the porosity.

The effective Young's modulus of a bar vibrating in its first flexural mode is [7]

$$E_{eff} = \rho_{exp} \left(0.975 f \frac{l^2}{t} \right)^2$$

where f is the vibration frequency and l and t are the length and the thickness of the sample, respectively. For our sample, $l = 29.3 \pm 0.2 \text{ mm}$, $t = 0.94 \pm 0.01 \text{ mm}$, $\rho_{exp} = (2520 \pm 80) \text{ kg m}^{-3}$ and $P \sim 41\%$. We obtained $E'_{eff}(T = 300 \text{ K on cooling}) = 3.4 \text{ GPa}$, $E'_{eff}(T = 291.5 \text{ K on cooling}) = 3.1 \text{ GPa}$, $E'_{eff}(T = 300 \text{ K on heating}) = 4.2 \text{ GPa}$, $E'_{eff}(T = 170 \text{ K}) = 6.0 \text{ GPa}$ and $E'_{eff}(T = 380 \text{ K}) = 3.6 \text{ GPa}$. Each one of these values has an uncertainty of $\sim 8\%$ and they must be corrected considering the porosity of the material. We used the model proposed by Mackenzie [15], which was proved to be quite good for the corrections to the longitudinal and shear velocities of the $\text{YBa}_2\text{Cu}_3\text{O}_{7-\delta}$ compound due to the porosity [16]. According to that model [15], the effective bulk and shear moduli, K and G respectively, and the void-free moduli, K_1 and G_1 , are linked by the following relationship:

$$\frac{1}{K} = \frac{1}{K_1(1-P)} + \frac{3P}{4G_1(1-P)}.$$

In an isotropic medium, such as a polycrystal, $G = \frac{E}{2(1+\nu)}$ and $K = \frac{E}{3(1-2\nu)}$ [7], so the Young's modulus, E'_1 , of a void-free sample is

$$E'_1 = E_{eff} \frac{(2 - 4\nu + P + P\nu)}{2(1 - 2\nu)(1 - P)}.$$

Considering the same value ($\nu = 0.3$) as used by Sugiyama *et al* [8], we obtained for our sample $E'_1(T = 300 \text{ K on cooling}) = 9.6 \text{ GPa}$, $E'_1(T = 291.5 \text{ K on cooling}) = 8.8 \text{ GPa}$, $E'_1(T = 300 \text{ K on heating}) = 11.9 \text{ GPa}$, $E'_1(T = 170 \text{ K}) = 16.9 \text{ GPa}$ and $E'_1(T = 380 \text{ K}) = 10.2 \text{ GPa}$. These values are considerably lower than that obtained by Sugiyama *et al* [8]; however, it must be considered that the chemical composition of the sample investigated by those authors is different from ours, as already pointed out in the previous section.

3.3. The anelastic relaxation in the orthorhombic phase

The anelastic spectrum of LiMn_2O_4 measured at two vibration frequencies below 250 K starting from the low-temperature state is reported in figure 4. An intense thermally activated peak is clearly visible at about 100 K, for a vibration frequency of the order of 1 kHz. To obtain the physical parameters of this process we tried to fit the peak by means of the Debye model. The contribution of a relaxation process to the dynamic Young's modulus is given by [7]

$$\begin{bmatrix} Q^{-1} \\ \delta E'/E' \end{bmatrix} = E\nu_0 c (\lambda_1 - \lambda_2)^2 \frac{1}{T} \frac{1}{\cosh^2\left(\frac{\Delta E}{2k_B T}\right)} \frac{1}{1 + (\omega\tau)^{2\alpha}} \begin{bmatrix} (\omega\tau)^\alpha \\ -1 \end{bmatrix} \quad (1)$$

where c is the molar concentration of relaxing units; λ_1 and λ_2 are the elastic dipoles in the two possible configurations 1 and 2 between which the relaxation can occur with a characteristic

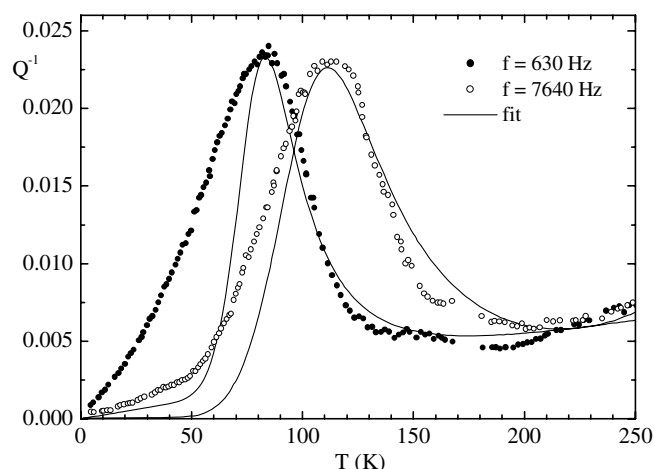


Figure 4. The elastic energy loss coefficient spectrum of LiMn_2O_4 measured at two vibrational frequencies below room temperature and best-fit curves with the Fuoss–Kirkwood model.

time $\tau(T)$ which generally follows an Arrhenius law, $\tau = \tau_0 \exp(E_a/kT)$; v_0 is the cell volume; ΔE is the asymmetry of the double potential well and $\alpha \equiv 1$. The contribution of a relaxation process to the absorption is a peak whose maximum is centred at the temperature at which $\omega\tau = 1$. Since τ is a decreasing function of temperature, the peak shifts to higher temperature if measured at higher ω . Around the same temperature, the real part of the Young's modulus presents a negative step. The Debye formula describes a relaxation process between two possible states which occurs with a single activation energy, E_a , and a single relaxation time, τ . Often real processes, like the one observed in LiMn_2O_4 , are broader than Debye peaks; in those cases a correction factor, α , is introduced in equation (1) (the Fuoss–Kirkwood model [7]). Physically, this means that the relaxation process has a distribution of activation energies and relaxation times which become broader as α decreases.

In figure 4 the best-fit curves obtained using the Fuoss–Kirkwood model are reported. A smooth background was considered. The best-fit parameters of the peak are: $\tau_0 \sim 4 \times 10^{-8}$ s, $E_a \sim 720$ K, $\Delta E \sim 80$ K and $\alpha \sim 0.75$. It can be noticed that whilst the high-temperature side of the peak can be quite well reproduced by these parameters, the low-temperature-side fit is not satisfactory. Although we cannot completely reproduce the peak, the parameters of the Fuoss–Kirkwood model fit provide an idea of the physical parameters of the process. A thermally activated anelastic peak at about 60 K with $E_a \sim 600$ K and $\tau_0 \sim 4 \times 10^{-11}$ s was measured by means of ultrasonic attenuation in a Fe_3O_4 single crystal and in similar compounds [7, 17]. It was attributed to stress-induced relaxations in the distribution of Fe^{2+} and Fe^{3+} ions occurring as a result of the transmission of ultrasonic waves. This conclusion was supported by the coincidence of the anelastic peak's activation energy with the activation energy of the electron hopping process which determines the electrical conduction in the same range of temperature in Fe_3O_4 . Fe_3O_4 and LiMn_2O_4 undergo a similar charge order transition and below this phase transition they both present a similar anelastic peak. It is likely that the origin of such peaks is the same—that is, the relaxation of one electron between two ions with a different charge. Unfortunately, to our knowledge, electrical conductivity measurements are not available below 240 K for LiMn_2O_4 , because at this temperature ρ has already attained the value of $3 \times 10^6 \Omega \text{ cm}$ [8, 10], and a direct comparison of the activation energy of the anelastic peak with that for hopping cannot be performed. Above 240 K the activation energy deduced from $\rho(T)$ is about 1700 K [8, 10], a value higher than that obtained for the activation

energy of the anelastic peak. However, at least in the case of Fe_3O_4 , the activation energy decreases as T decreases [2]. One can speculate that in LiMn_2O_4 also, the activation energy for the hopping process decreases with decreasing T and finally can coincide with E_a for the anelastic peak. Fe_3O_4 and LiMn_2O_4 show a marked difference in relaxation time, τ_0 , of the relaxation in the charge ordered state. This can be explained considering that magnetite has an electrical resistivity at least five orders of magnitude lower than that of LiMn_2O_4 [10], so electron exchange between Mn^{3+} and Mn^{4+} occurs less frequently than in Fe_3O_4 , explaining the longer τ_0 . The extremely high value of τ_0 for LiMn_2O_4 (4×10^{-8} s), is quite different from the typical times for the relaxation of a point defect (10^{-14} – 10^{-13} s). However, it must be considered that electrons in this compound are not free charges but are more likely polarons [1] which can move only transporting a big lattice distortion, so the time needed to relax a defect into a different state can become quite long.

Another possible origin of the anelastic peak of LiMn_2O_4 around 100 K comes from the analogy of the crystal structure of this compound with that of HTSCs. In HTSCs there are interconnected CuO_6 octahedra sharing corners with the others. Anelastic measurements [18, 19] and joint anelastic spectroscopy and NMR measurements [20] of $\text{La}_2\text{CuO}_{4+\delta}$ indicated that CuO_6 octahedra can tilt between four equivalent positions, giving rise to strong thermally activated peaks in the anelastic spectrum centred around 150 K for a measurement frequency of about 1 kHz. Moreover, at low temperature the oxygen octahedra can tilt due to quantum tunnelling [18, 19]. The parameters of the classical thermally activated peak are $E_a = 2800$ K, $\tau_0 = 2 \times 10^{-12}$ s, $\alpha = 0.46$. Also the structure of LiMn_2O_4 can be decomposed into MnO_6 octahedra and LiO_4 tetrahedra, as reported in figure 1. It is possible also that, in the spinel structure, small movements of these polyhedra can take place, giving rise to a strong anelastic peak.

4. Conclusions

We measured the anelastic spectrum of LiMn_2O_4 between 1 and 400 K. It confirms the occurrence of a first-order phase transition around room temperature, characterized by a large hysteresis and the coexistence of two phases. The shape of the real part of the Young's modulus seems to indicate that the elastic constant which is more strongly affected by the transition is c_{44} , like in the case of Fe_3O_4 . The time evolution of E' in the coexistence region was measured. It can be quite satisfactorily fitted by an exponential law. The characteristic time of this evolution rapidly decreases from 296 to 290 K and then increases at 289 K. The change of this time constant with T can be related to the temperature behaviour of E' . A procedure to estimate the absolute value of the Young's modulus of the sample considering the effect of its porosity is presented. We obtained E' of the order of 10 GPa. Finally, around 100 K we revealed a thermally activated peak, which can be ascribed to an electron exchange between Mn^{3+} and Mn^{4+} , through the analogy with Fe_3O_4 , or to little movements of the octahedra and tetrahedra composing the crystal structure, through the analogy with HTSCs.

Acknowledgment

The authors thank F Cordero for useful discussions and for a critical review of the manuscript.

References

- [1] Rodriguez-Carvajal J, Rousse G, Masquelier C and Hervieu M 1998 *Phys. Rev. Lett.* **81** 4660
- [2] Verwey E J W 1939 *Nature* **144** 327

- [3] Wright J P, Attfield J P and Radaelli P G 2001 *Phys. Rev. Lett.* **87** 266401
- [4] Rousse G, Masquelier C, Rodriguez-Carvajal J and Hervieu M 1999 *Electrochem. Solid State Lett.* **2** 6
- [5] Paolone A, Roy P, Rouse G, Masquelier C and Rodriguez-Carvajal J 1999 *Solid State Commun.* **111** 453
- [6] Rouse G, Masquelier C, Rodriguez-Carvajal J, Elkaim E, Lauriat J P and Martinez J L 1999 *Chem. Mater.* **11** 3629
- [7] Nowick A S and Berry B S 1972 *Anelastic Relaxation in Crystalline Solids* (New York: Academic)
- [8] Sugiyama J, Tamura T and Yamauchi H 1995 *J. Phys.: Condens. Matter* **7** 9755
- [9] Oikawa K, Kamiyama T, Izumi F, Chakoumakos B C, Ikuda H, Wakihara M, Li J and Matsui Y 1998 *Solid State Ion.* **109** 35
- [10] Shimakawa Y, Numata T and Tabuchi J 1997 *J. Solid State Chem.* **131** 138
- [11] Schwenk H, Bareiter S, Hinkel C, Lüthi B, Kakol K, Koslowski A and Honig J M 2001 *Eur. Phys. J. B* **13** 491 and references therein
- [12] Fine M E and Kenney N T 1954 *Phys. Rev.* **94** 1573
- [13] Nye J F 1957 *Physical Properties of Crystals* (London: Oxford University Press)
- [14] Mazenko G F and Zannetti M 1985 *Phys. Rev. B* **32** 4565
- [15] Mackenzie J K 1950 *Proc. Phys. Soc. B* **63** 2
- [16] Masi L, Borchi E and de Gennaro S 1996 *J. Phys. D: Appl. Phys.* **29** 2015
- [17] Kamigaki K 1961 *J. Phys. Soc. Japan* **16** 1170
- [18] Cordero F, Grandini C R, Cannelli G, Cantelli R, Trequatrini F and Ferretti M 1998 *Phys. Rev. B* **57** 8580
- [19] Cordero F, Cantelli R and Ferretti M 2000 *Phys. Rev. B* **61** 9775
- [20] Cordero F, Cantelli R, Corti M, Campana A and Rigamonti A 1999 *Phys. Rev. B* **59** 12078